Intramolecular and Lattice Melting in *n*-Alkane Monolayers: An Analog of Melting in Lipid Bilayers

F. Y. Hansen,[1] K. W. Herwig,[2,*] B. Matthies,[2,†] and H. Taub[2]
[1]*Department of Chemistry, Technical University of Denmark, IK·207·DTU, DK-2800 Lyngby, Denmark*
[2]*Department of Physics and Astronomy and Missouri University Research Reactor Facility, University of Missouri-Columbia, Columbia, Missouri 65211*
(Received 4 November 1998)

Molecular dynamics (MD) simulations and neutron diffraction experiments have been performed on *n*-dotriacontane (n-$C_{32}D_{66}$) monolayers adsorbed on a graphite basal-plane surface. The diffraction experiments show little change in the crystalline monolayer structure up to a temperature of ~350 K above which a large thermal expansion and decrease in coherence length occurs. The MD simulations provide evidence that this behavior is due to a phase transition in the monolayer in which intramolecular and translational order are lost simultaneously. This melting transition is qualitatively similar to the gel-to-fluid transition found in bilayer lipid membranes.

PACS numbers: 68.35.Bs, 61.12.–q, 64.70.–p, 87.16.–b

Intermediate-length *n*-alkane molecules [CH_3-$(CH_2)_{n-2}CH_3; 20 < n < 40$] adsorbed on solid substrates are of interest as prototypical systems for the interfacial behavior of more complex polymers [1–3] and, in their own right, as model systems for studies of lubrication [4]. Considerable progress has been made over the last 30 years in thermodynamic studies of these films [5,6]; and, more recently, in determining their structure by scanning tunneling microscopy [7,8] and diffraction techniques [9,10]. In contrast, the interfacial dynamics of these prototypical molecules is less well understood [11,12]. To begin such studies, we have undertaken investigations by both molecular dynamics (MD) simulations and neutron diffraction of the temperature dependence of their monolayer structure and melting transition.

Here we report some of our MD and neutron diffraction results on the melting behavior of *n*-dotriacontane (n-$C_{32}H_{66}$ hereafter referred to as C32) and *n*-tetracosane (n-$C_{24}H_{50}$ or C24) adsorbed on a graphite substrate. We propose that these monolayers melt via the same "footprint reduction" mechanism found for shorter alkane monolayers [13] whereby molecular motion perpendicular to the adsorbing surface creates vacancies in the monolayer which allow translational and rotational disorder to develop. We find, though, a new feature in the monolayer melting of these longer alkanes. The footprint reduction mechanism operative at melting involves a collective structural collapse of the molecules from a linear to a more globular shape. Thus the monolayer melting transition is qualitatively similar to the well-known gel-to-fluid transition in bilayer lipid membranes [14–16] in which intrachain and lattice melting occur simultaneously.

Before describing these melting studies, we summarize what is known about the solid structure of these films from recent neutron diffraction experiments on completely deuterated monolayers of C32 [10] and C24 [17]. When these monolayers are deposited from the vapor phase, they order, at room temperature, in the incommensurate rectangular-centered structure on the graphite (0001) surface shown in Fig. 1(a) in which each of the two sublattices forms rows of parallel molecules, the so-called lamellae. Both molecules in the unit cell are in the *trans* conformation and are oriented with their carbon skeletal plane parallel to the graphite surface. We refer to this structure as the "low-density" phase.

The diffraction experiments [10,17] have also shown that, if the same monolayer is deposited from an *n*-heptane solution (n-C_7D_{16}), a denser structure is formed commensurate with the graphite basal plane. In this "high-density" phase, the monolayer contracts in a direction parallel to the lamellae boundaries to a lattice constant $b = 4.26$ Å, and alternate molecules along this direction reorient so that their carbon skeletal plane is perpendicular to the surface as shown in Fig. 1(b) [18].

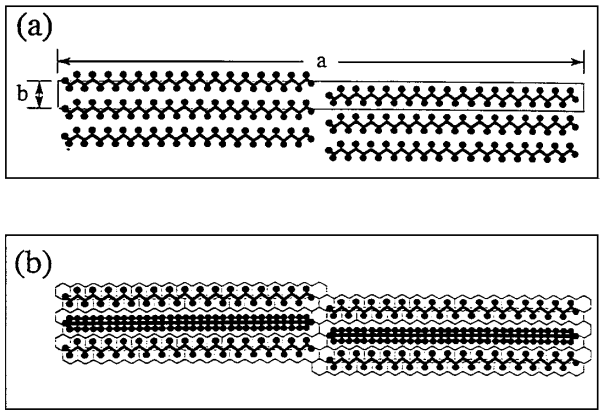

FIG. 1. Unit cells of n-$C_{32}D_{66}$ monolayers adsorbed on the graphite (0001) surface at room temperature: (a) vapor-deposited monolayer and (b) solution-deposited monolayer in which the molecules have alternating parallel and perpendicular orientations within a lamella. The honeycomb network in (b) is used to depict registry of the monolayer with the underlying graphite basal-plane surface.

 0031-9007/99/83(12)/2362(4)$15.00

To investigate the melting behavior of the low-density phase of both the C24 and C32 monolayers, we have measured their diffraction patterns as a function of temperature as shown for C32 in Fig. 2(a). The patterns were obtained at the Missouri University Research Reactor by the same method as described in Ref. [10]. Sample preparation techniques have been discussed in detail elsewhere [19]. The dominant feature in the diffraction patterns is the (11) Bragg peak whose position and width allow monitoring of the thermal expansion and coherence length of the monolayer in the **b** direction.

The patterns for the C32 monolayer in Fig. 2(a) show only a small shift of the (11) peak to lower wave vector transfer Q up to a temperature of about 350 K, indicating a slight thermal expansion. However, above this temperature, there is a much larger expansion and the peak broadens greatly. The diffraction patterns of the C24 monolayer (not shown) indicate a similar temperature dependence except that the large thermal expansion and peak broadening begins at about 340 K. This behavior is seen more easily in Fig. 2(b) which shows the temperature dependence of the coherence length in the **b** direction, L_b, and the b lattice constant obtained by fitting the diffraction patterns as in Ref. [10]. Note that L_b is inversely proportional to the leading half width at half maximum of the (11) peak.

In order to interpret microscopically the temperature dependence of the diffraction patterns, we have performed extensive MD simulations of both the low- and high-density phases of monolayer C32 by a method similar to that used in our previous simulations of n-butane ($n = 4$) and n-hexane ($n = 6$) monolayers on graphite [13,20].

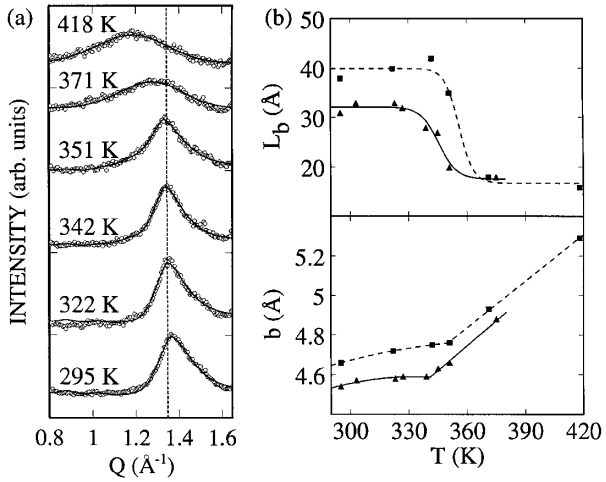

FIG. 2. (a) Temperature dependence of the (11) Bragg peak in neutron diffraction patterns from a vapor-deposited monolayer of n-$C_{32}D_{66}$ on a Grafoil substrate. The solid curves are guides to the eye, and the dashed vertical provides a fiducial line for gauging the peak shift. (b) Temperature dependence of the coherence length in the **b** direction (top panel) and lattice constant b (lower panel) for the n-$C_{32}D_{66}$ monolayer (squares) and n-$C_{24}D_{50}$ monolayer (triangles).

This method employs a canonical sampling scheme (constant volume, temperature, and a fixed number of molecules). The alkane molecules are represented by a unified atom model in which the methyl and methylene groups are replaced by pseudoatoms of their respective masses at the carbon atom position, and the pseudoatom separation is constrained to the C-C bond length of 1.53 Å. Molecular flexibility is retained by allowing dihedral torsional motion about the C-C bond as well as the C-C-C angle-bending motion. We used the same intermolecular and intramolecular potentials as previously [13,20] except for the atom-substrate potential where we have substituted the parameters of Velasco and Peters [21]. Their simulations gave better agreement with the melting temperatures observed for butane and hexane monolayers [22].

Of particular concern in the computations is the choice of the simulation cell dimensions. For melting studies it is important that the simulations accurately reproduce the monolayer spreading pressure and lattice constants. Furthermore, the simulation cell must retain the translational symmetry of the graphite basal plane. To satisfy these requirements with a simulation cell size small enough to permit feasible computation times, we have assumed that the incommensurate low-density structure corresponds to an unconstrained film with zero spreading pressure at low temperature. The simulation cell for the C32 monolayer contains 32 molecules which, in the initial configuration, are oriented as shown in Fig. 1(a). Most of the data reported below are from an 800–1000 ps time block when the system appears to be equilibrated. Close to the melting transition, where equilibration times are longer, the simulation times are typically 1500–2000 ps. The simulation of the low-density C32 system at 20 K and zero spreading pressure equilibrated with nearly all molecules in their initial configuration.

To characterize the system at higher temperatures, it is helpful to consider the intermolecular and intramolecular potential energies per molecule plotted in Fig. 3. The intermolecular potential, E_{inter}, is the pairwise interaction energy between pseudoatoms in different molecules summed up to a cutoff length of 10 Å, while the intramolecular potential, V_{intra}, is the sum of the bond-angle and dihedral-torsion energies within all of the molecules. V_{intra} takes on its minimum value in the ordered state when all dihedral bonds are in the *trans* configuration and increases as disorder in the form of *gauche* defects appears in the chains.

In Fig. 3, we see that *both* the intermolecular and intramolecular energies have an inflection point at the same temperature of ~350 K in good agreement with the onset temperature for the large thermal expansion and loss of coherence observed in the diffraction experiment. We interpret this behavior as resulting from the simultaneous appearance of both intermolecular and intramolecular disorder at the melting point of the C32 monolayer.

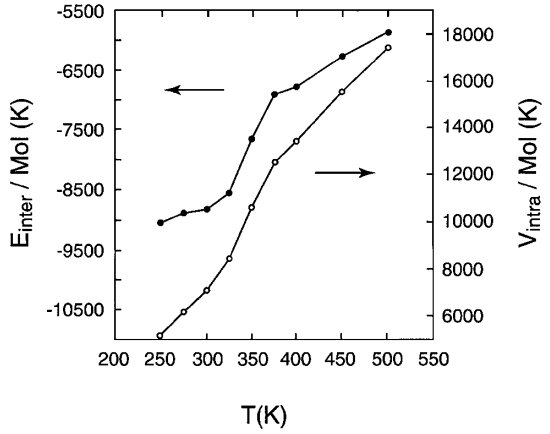

FIG. 3. Temperature dependence of the intermolecular (E_{inter}, filled circles) and intramolecular (V_{intra}, open circles) potential energies per molecule as defined in the text and calculated from the MD simulations of the low-density C32 monolayer phase.

In support of this interpretation, we have also calculated from the simulations the probability that each of the 29 dihedral bonds in a C32 molecule is in a *gauche* conformation. The results are shown in Fig. 4(a). We see that the distributions have a similar form at all temperatures characterized by a plateau of a relatively small level of defects in the middle of a molecule with a higher number of defects toward its ends. Moreover, the height of the plateau in the defect distribution increases much more rapidly in the temperature range 325 to 375 K than it does either above or below this range so that the distribution at 350 K appears separated from the others. The MD simulations also show a rapid decrease in the average end-to-end distance of the molecules in this temperature range. Thus we identify a transition point at ~350 K between a low-temperature phase in which there is a relatively small number of chain defects and a high-temperature phase in which there is a high level of defects. The fact that this transition occurs at the same temperature as the inflection point in E_{inter} is consistent with our interpretation that intramolecular and translational order are lost simultaneously in the monolayer. The MD simulations of the high-density C32 monolayer phase give qualitatively the same results as those described above for the low-density system but with a lower melting point of 325 K.

The distribution of *gauche* defects within the molecule and the C32 monolayer melting transition have an interesting analog in systems of lipid molecules forming bilayer membranes. These membrane-forming molecules consist of a large ionic hydrophilic headgroup with two alkane chains of typically 12–18 carbon atoms depending on the molecule. In a bilayer membrane, the headgroups are located at its two outer surfaces with the alkane chains meeting in the hydrophobic membrane interior. At low temperature, the axes of the alkane chains are aligned perpendicular to the plane of the membrane with most of the dihedral bonds in the *trans* configuration. The chain axes

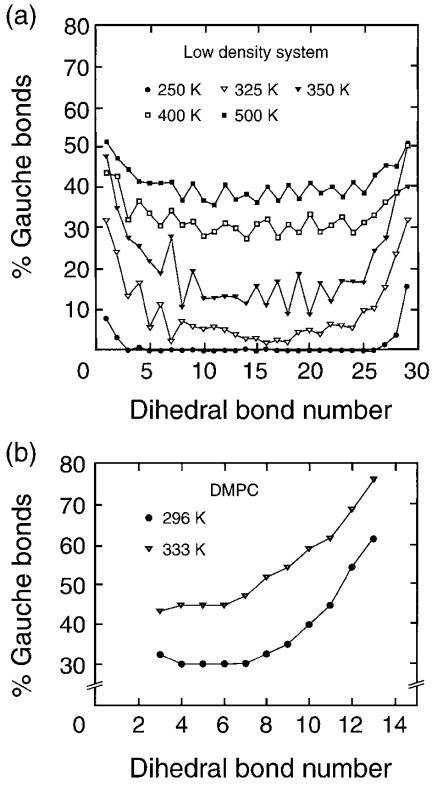

FIG. 4. (a) Temperature dependence of the distribution of *gauche* defects along the C32 chains in the low-density phase; (b) distribution of *gauche* defects along the alkane chains in the bilayer-lipid membrane dimyristoyl phosphatidylcholine (DMPC) at low temperatures from Ref. [16]. The gel-to-fluid transition is at 296 K.

are typically arranged in a hexagonal pattern forming the so-called gel phase.

Upon heating, the gel phase is known to undergo a transition to an isotropic fluid in which the hexagonal lattice order is lost simultaneously with the intrachain order. Disorder within the chains can be described by a characteristic distribution of *gauche* defects along their length as shown at two temperatures in Fig. 4(b) for a bilayer membrane of the lipid dimyristoyl phosphatidylcholine (DMPC). This molecule has 14 carbon atoms in its alkane chains [16], and the probability of a *gauche* defect at each C-C bond has been determined experimentally by NMR using a method originally developed by Seelig and Seelig [14,15]. Since the method relies on the dynamic exchange between *trans* and *gauche* states, the distribution can be measured only in the fluid phase of the membrane where this exchange is sufficiently rapid.

If we cut the distributions of *gauche* defects shown in Fig. 4(a) at the midpoint of the C32 molecule to break the symmetry absent in the membrane-forming molecule, then the distributions can be compared with those of the DMPC chains in Fig. 4(b). Despite the qualitatively different structure of the C32 monolayer and the DMPC bilayer, the *gauche* defect distributions in the high-temperature C32

monolayer phase and the DMPC fluid are qualitatively similar. We conclude that in both systems a collective transition is occurring in which both intrachain and lattice order are lost.

The MD simulations on C24 and C32 monolayers together with those of shorter alkanes on a graphite surface provide additional evidence that the rapid increase in *gauche* defects within the molecules is not occurring simply as a result of the thermal expansion which accompanies the monolayer melting. Simulations of a hexane monolayer (n-C_6H_{14}) also showed *gauche* defects appearing in the molecules below the melting transition at 175 K [13,20]. Furthermore, we could demonstrate their role in driving the melting transition by tripling the height of intramolecular *trans-gauche* energy barrier so that no *gauche* defects could be formed. This resulted in an increase in the monolayer melting point by $\sim$75 K. We expect a similar behavior to occur in monolayers of the longer C24 and C32 molecules and have therefore not checked this explicitly. Instead, we conducted another test to determine whether lattice melting is driving the generation of *gauche* defects. In a simulation at 400 K, all intermolecular interactions were switched off while still including the holding potential of the C32 molecules on the graphite substrate. This yielded a qualitatively different shape of the *gauche* defect distribution from those in Fig. 4(a). The fraction of *gauche* bonds was nearly constant throughout the length of the molecule and at a *lower* level of $\sim$10% compared to a plateau of $\sim$30% in the central region of the molecules found with the intermolecular interaction present. If *gauche* defects were appearing in the molecules due to expansion of the lattice in the high-temperature fluid phase, we would have expected their number to increase rather than decrease in a simulation of noninteracting molecules.

In summary, we have found evidence of a phase transition in monolayers of intermediate-length alkane chains adsorbed on a graphite surface which exhibits a chain-melting transition in conjunction with lattice melting similar to that found in bilayer lipid membranes. As simpler systems consisting of a single layer of molecules without headgroups, the alkane monolayers facilitate a more detailed study of the dynamics through the melting transition both experimentally and by MD simulation. In particular, quasielastic neutron scattering experiments are now in progress for comparison with the simulations.

Acknowledgment is made to the U.S. National Science Foundation under Grants No. DMR-9314235 and No. DMR-9802476, the Missouri University Research Reactor, and to the donors of The Petroleum Research Fund, administered by the ACS, for partial support of this research. We thank L. Criswell for assistance with the figures.

*Present address: Intense Pulsed Neutron Source, Building 360, Argonne National Laboratory, Argonne, Illinois 60439-4814.

†Present address: The Goodyear Tire and Rubber Company, Corporate Research Division, 142 Goodyear Boulevard, Akron, Ohio 44305.

[1] See, e.g., P. G. de Gennes, Adv. Colloid Interface Sci. **27**, 189 (1987).

[2] J. N. Israelachvili, *Intermolecular and Surface Forces* (Academic Press, London, 1985).

[3] S. Granick, Science **253**, 1374 (1991).

[4] M. Mondello and G. S. Grest, J. Chem. Phys. **103**, 7156 (1995).

[5] A. J. Groszek, Proc. R. Soc. London A **314**, 473 (1970).

[6] G. H. Findenegg and M. Liphard, Carbon **25**, 119 (1987).

[7] G. C. McGonigal, R. H. Bernhardt, and D. J. Thomson, Appl. Phys. Lett. **57**, 28 (1990).

[8] J. P. Rabe and S. Buchholz, Science **253**, 424 (1991).

[9] K. Morishige, Y. Takami, and Y. Yokota, Phys. Rev. B **48**, 8277 (1993).

[10] K. W. Herwig, B. Matthies, and H. Taub, Phys. Rev. Lett. **75**, 3154 (1995).

[11] S. Granick, in *Physics of Polymer Surfaces and Interfaces*, edited by I. C. Sanchez (Butterworth-Heinemann, Boston, 1992), p. 227.

[12] T. K. Xia and U. Landman, Science **261**, 1310 (1993).

[13] F. Y. Hansen and H. Taub, Phys. Rev. Lett. **69**, 652 (1992); F. Y. Hansen, J. C. Newton, and H. Taub, J. Chem. Phys. **98**, 4128 (1993).

[14] A. Seelig and J. Seelig, Biochemistry **13**, 4839 (1974).

[15] J. Seelig, Q. Rev. Biophys. **10**, 353 (1977).

[16] J.-P. Douliez, A. Léonard, and E. J. Dufourc, Biophys. J. **68**, 1727 (1995).

[17] B. Matthies, K. W. Herwig, L. Criswell, H. Taub, and F. Y. Hansen (to be published).

[18] More precisely, the profile analysis of the diffraction pattern favors approximately equal numbers of parallel and perpendicular oriented molecules. Potential energy calculations, in which the b lattice constant is fixed at 4.26 Å, yield the lowest energy for monolayer clusters with an alternating parallel/perpendicular configuration.

[19] K. W. Herwig, B. Matthies, and H. Taub, in *Neutron Scattering in Materials Science*, edited by D. A. Neumann, T. P. Russell, and B. J. Wuensch, MRS Symposia Proceedings No. 376 (Materials Research Society, Pittsburgh, 1994), p. 757.

[20] K. W. Herwig, Z. Wu, P. Dai, H. Taub, and F. Y. Hansen, J. Chem. Phys. **107**, 5186 (1997).

[21] E. Velasco and G. H. Peters, J. Chem. Phys. **102**, 1098 (1995). For the atom-substrate potential, we use their Lennard-Jones parameters $\sigma = 3.66$ Å and $\varepsilon = 45.0$ K.

[22] H. Taub, in *The Time Domain in Surface and Structural Dynamics*, edited by G. J. Long and F. Grandjean, NATO Advanced Study Institutes, Ser. C, Vol. 228 (Kluwer, Dordrecht, 1988), p. 467.